Available online at www.sciencedirect.com

ScienceDirect

Ceramics International 40 (2014) 2669–2675

CERAMICS INTERNATIONAL

www.elsevier.com/locate/ceramint

Microstructure and optical limiting properties of multicomponent inorganic gel-glasses: A focus on SiO_2, TiO_2 and PbO gel-glasses

Zheng Chan*, Li Wei, Chen Wenzhe, Ye Xiaoyun, Cai Shuguang, Xiao Xueqing

College of Materials Science and Engineering, Fujian University of Technology, 3 Xuefu Road, Fuzhou 350108, PR China

Received 12 September 2013; accepted 14 October 2013
Available online 21 October 2013

Abstract

Two kinds of multicomponent inorganic gel-glasses, namely, SiO_2–TiO_2 binary and SiO_2–TiO_2–PbO ternary gel-glasses, were obtained via the hydrolysis and co-condensation of tetraethyloxysilane ($Si(OC_2H_5)_4$, TEOS), titanium tetraisopropoxide ($Ti(C_4H_9O)_4$, TTIP), and lead (II) acetate trihydrate ($Pb(Ac)_2$). X-ray diffraction, scanning electron microscopy, Fourier transform infrared spectroscopy, thermogravimetric analysis, and pore structure measurements were performed to investigate the morphology, structure, and texture properties of the gel-glasses. The samples were mainly composed of amorphous phase without any detected phase separation. The introduced Ti^{4+} and Pb^{2+} were partially involved in the hydrolysis and condensation processes. Furthermore, the composition had a significant influence on the pore structure of silica-based gel-glasses, and the introduction of TiO_2 in the gel-glasses caused the formation of bimodal-distributed pore shapes and dimensions in multicomponent inorganic gel-glasses. The optical limiting (OL) properties were measured at 532 nm by using the open aperture Z-scan technique. The SiO_2–TiO_2 binary and SiO_2–TiO_2–PbO ternary gel-glasses exhibited greatly enhanced OL behaviors than the SiO_2 unitary gel-glass. The observed OL phenomenon in the SiO_2–TiO_2 binary gel-glass originated from two-photon absorption (TPA), whereas TPA followed by nonlinear scattering (NLS) contributed to the increased OL performance of the SiO_2–TiO_2–PbO ternary gel-glass. SiO_2–TiO_2 binary and SiO_2–TiO_2–PbO ternary gel-glasses are potential materials for practical applications in the fields of optics, all-optical switching, and related optical devices.

Keywords: A. Sol–gel process; Microstructure; Optical limiting; Nonlinear optical

1. Introduction

Optical limiters (OLs) have received increasing interest in the past decade. OLs can effectively attenuate intense and potentially dangerous laser beams, and only allow a reduced transmission to the target area while exhibiting high-transmittance at low ambient light. Moreover, OLs are capable of protecting human eyes and optical sensors from damages [1–6]. A number of materials, such as fullerenes [1], phthalocyanines (Pcs) [2], porphyrins [2], carbon nanotubes [3], graphene [4], metal nanoparticles [5], and semiconductor nanoparticles [6], among others, have presented strong nonlinear extinction for high-intensity light and hence could be considered as potential optical-limiting materials. For practical use, OL materials should be introduced into a solid matrix for the fabrication of devices.

Given their high optical quality and freedom to be impregnated with various additives to modify their optical characteristics, pure inorganic sol–gel materials, such as SiO_2, have been widely investigated for optical applications, including optical waveguides and OLs. In our previous works, phthalocyanines, carbon nanotubes (CNTs), and silver nanoparticles were successfully incorporated into silica glass via the sol–gel technique [7–9]. The experimental results indicate that the original OL performances of the doping components were maintained or even enhanced after being introduced into the solid-state matrix, thereby confirming that sol–gel-derived silica glasses are viable host candidates for OL materials. However, several urgent issues regarding solid-state OL composites, such as the dimer behavior of Pcs, aggregation of CNTs, and instability of metal nanoparticles during the sol–gel procedure that would significantly influence the OL performance of the doped components,

*Corresponding author. Tel./fax: +86 591 2286 3279.
E-mail address: czheng.fjut@gmail.com (C. Zheng).

0272-8842/$ - see front matter © 2013 Elsevier Ltd and Techna Group S.r.l. All rights reserved.
http://dx.doi.org/10.1016/j.ceramint.2013.10.057

remain to be solved. Situ synthesis is proposed to overcome with such problems. However, the structure, morphology, and distribution of doping OL materials are difficult to control precisely, and the resulting composites typically exhibit weak OL properties. In fact, if the mother matrix itself can produce OL behavior by introducing some transition metal ions and/or heavy metal ions, which participate in the hydrolysis and polycondensation, to obtain binary or ternary gel-glasses, then particular novel and interesting OL properties may be obtained. Unfortunately, to the best of our knowledge, only a few studies have investigated the OL behavior of binary and ternary gel-glasses, even though it is of fundamental importance to the development of practical applications and exploration of new materials in the field of nonlinear optics.

In this study, Ti^{4+} and Pb^{2+} were chosen as representatives of transition metal and heavy metal ions, respectively, to prepare SiO_2–TiO_2 binary and SiO_2–TiO_2–PbO ternary gel-glasses via the sol–gel technique. The structure and texture of the gel-glasses were traced via X-ray diffraction (XRD), scanning electron microscopy (SEM), FT-IR spectroscopy, thermogravimetric analysis (TGA), and pore structure measurements. In addition, the OL properties were investigated at the laser wavelength of 532 nm via the open Z-scan method.

2. Experimental

2.1. Sample preparation

All chemicals were used as received. Tetraethoxysilane (Si$(OC_2H_5)_4$, TEOS), titanium tetraisopropoxide (Ti$(C_4H_9O)_4$, TTIP), lead (II) acetate trihydrate (Pb$(Ac)_2$), 2-methoxyethanol anhydrous, acetic acid, acetylacetone (acac), N-N′ dimethyl formamide (DMF), and HNO_3 were obtained from the Chinese Reagent Corporation and were of analysis grade.

Molar ratio of (R+TEOS):ethanol:distilled water in the precursor was 1:5:5 (R=TTIP, (TTIP+Pb$(Ac)_2$)). DMF was introduced in a proportion of 0.5 DMF/ethanol volume ration, and was used as both solvent and drying control chemical additive. A molar ratio of R/TEOS of 2:8 was chosen because our previous work has shown that this is the optimum ratio in terms of texture and optical transparency. In addition, the molar ratio of TTIP to Pb$(Ac)_2$ is 1:1 in ternary gel-glass. For comparison, unitary silica gel-glass was also prepared. Specially, the required TEOS, ethanol, DMF, and aqueous were first stirred for 30 min to obtain a homogeneous solution of precursor I. The required proportion of TTIP was then dissolved in acetylacetone for the case of SiO_2–TiO_2, and TTIP+Pb$(Ac)_2$ was dissolved in the mixture of 2-methoxyethanol anhydrous, acetic acid, and acetylacetone for the case of SiO_2–TiO_2–PbO to obtain precursor II. Subsequently, precursors I and II were mixed by stirring, and a small amount of HNO_3 was then added dropwise to promote hydrolysis (pH=5–6). The resulting clear sol was continuously stirred for another 24 h at room temperature, and the mixture was then divided into several equal volume parts, cast into polystyrene cells individually, sealed, and left to age and dry for 6 months. When the mass of the samples remained constant, final gel-glasses with two smooth, parallel surfaces and a unit thickness of 1 mm were obtained, and optical characterization without further handling can be performed on these samples. The obtained SiO_2–TiO_2 and SiO_2–TiO_2–PbO gel-glasses were transparent to the human eye and had linear transmittances of 46.48% and 43.63%, respectively.

2.2. Characterization

X-ray diffraction patterns were obtained using a Bruker D8 advanced diffractometer with Cu Kα radiation of k=1.54056 Å. The morphologies of the gel-glasses were observed using a field-emission SEM (JSM-6700, JEOL Ltd.). In the SEM investigation, gold was deposited onto the freshly fractured surface of the sample via sputtering. FT-IR spectra were obtained using a Thermo NICOLET 6700 spectrometer. The samples were prepared in the form of KBr pellets. TGA was performed using a NETZSCH STA 449 F3 thermal analysis instrument (heating rate of 10 deg/min, nitrogen atmosphere protection). Data in the range of 25 °C to 1000 °C were collected. N_2 absorption-desorption isotherms were measured at 77 K by using a Belsorp-Max Surface Area and Porosimetry analyzer. The samples were degassed at 393 K for 12 h prior to measurements.

2.3. Z-scan measurements

The OL properties of the SiO_2, SiO_2–TiO_2, and SiO_2–TiO_2–PbO gel-glasses were investigated via an open-aperture Z-scan technique [10] by using 4 ns laser pulses from a Nd:YAG laser (Brio 640) at a repetition rate of 1 Hz and a wavelength of 532 nm. The pulse energies in front of and behind the samples were monitored using energy detectors D1 and D2 (Ophir Optronics Inc. PE25). The forward-scattered energy was recorded using D3 (Ophir Optronics Inc. PD10) at an angular position of 45° relative to the laser direction. The outputs recorded by the detectors were fed into a computer through a Laserstar-Dual-Channel-Display (Ophir Optronics Inc.). The laser beam waist was set at approximately 14.5 μm, and the energy of a single pulse was set at 200 μJ. All measurements were conducted at room temperature. The gel-glasses were fixed vertically using a clamp. Each sample was mounted on a computer-controlled translation stage that translated the sample along the Z-axis.

3. Results and discussion

3.1. Structural studies

The XRD patterns of the as-prepared SiO_2, SiO_2–TiO_2, and SiO_2–TiO_2–PbO gel-glasses shown in Fig. 1 did not exhibit sharp peaks, which indicate the non-crystalline nature of the materials. Fig. 2 shows the surface microstructure of the SiO_2 and SiO_2–TiO_2 gel-glasses (SiO_2–TiO_2 and SiO_2–TiO_2–PbO gel-glasses share the same surface morphology, and thus, only the image of SiO_2–TiO_2 is presented as representative). In Fig. 2, both gel-glasses were composed of round-like

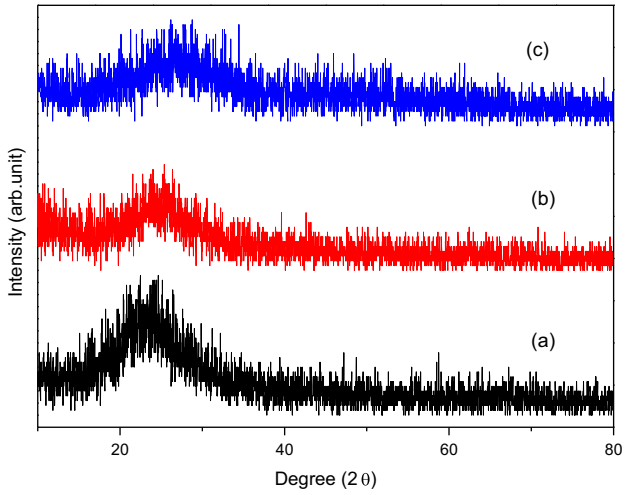

Fig. 1. X-ray diffraction patterns of (a) SiO_2, (b) SiO_2–TiO_2, and (c) SiO_2–TiO_2–PbO gel-glasses.

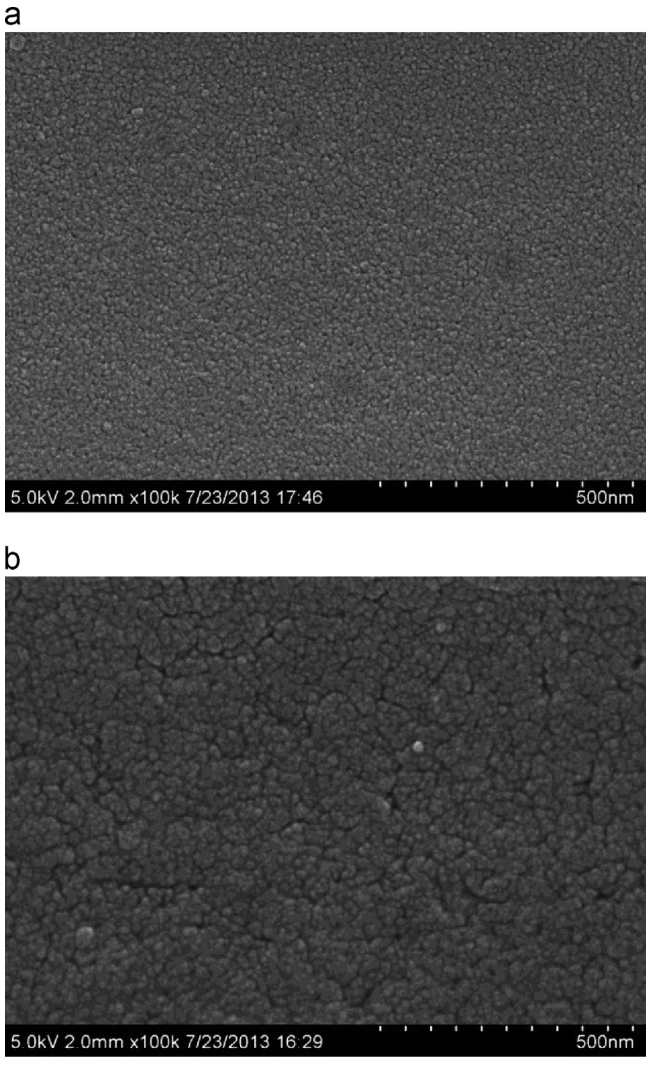

Fig. 2. Micro-morphologies of the (a) SiO_2 and (b) SiO_2–TiO_2 gel-glasses.

nanoparticles or aggregates. The granules of the SiO_2–TiO_2 gel-glass were larger and its surface was less condensed compared with those of the SiO_2 gel-glass.

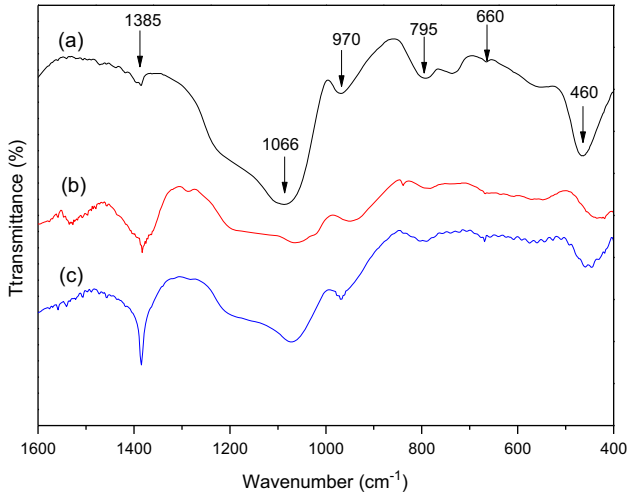

Fig. 3. FT-IR spectra of the (a) SiO_2, (b) SiO_2–TiO_2, and (c) SiO_2–TiO_2–PbO gel-glasses.

FT-IR spectroscopy is a powerful tool used for investigating structural changes in sol–gel-derived glasses. Fig. 3 shows the low wave number region of the FT-IR absorption spectra of the SiO_2–TiO_2 and SiO_2–TiO_2–PbO gel-glasses; the spectrum of the SiO_2 gel-glass is also presented for comparative purposes. The SiO_2 gel-glass exhibited four fundamental absorption bands at 1066, 795, 660, and 460 cm^{-1}, which originated from the anti-symmetric stretching vibration of Si–O–Si, symmetric stretching vibration of the Si–O–Si, ring vibrations of [SiO_4] tetrahedral units, and asymmetrical bending vibration of Si–O–Si, respectively [11]. Another band was observed at 970 cm^{-1}, which corresponds to the vibration of Si–OH groups and is a byproduct of the incomplete condensation of silanes. In the SiO_2–TiO_2 and SiO_2–TiO_2–PbO gel-glasses, the intensity of the band centered at 1385 cm^{-1} increased because of the Ti–O–C vibration generated by the Ti-acac chelates [12]. Furthermore, an additional band at approximately 453 cm^{-1} was observed and can be attributed to the Ti–O stretching vibration [13]. The SiO_2–TiO_2–PbO gel-glass exhibited a weak visible absorption peak at approximately 430 cm^{-1} [14], which is broader than the band of asymmetrical bending vibration of Si–O–Si. This weak peak is induced by the P–O vibration in the [PbO_4] group. In addition, the intensity of the bands induced by the Si–O–Si vibration in the SiO_2 gel-glass was lower than that of the SiO_2–TiO_2 and SiO_2–TiO_2–PbO gel-glasses, which suggests that the introduced Ti^{4+} and Pb^{2+} were partially involved in the hydrolysis and condensation processes.

3.2. Thermal studies

Fig. 4 shows the typical TGA curves of the SiO_2, SiO_2–TiO_2, and SiO_2–TiO_2–PbO gel-glasses. The three TGA curves can be roughly divided into three stages. In the first stage, which was conducted from room temperature to 150 °C, mass losses of approximately 8.23%, 11.56%, and 12.47% in the SiO_2, SiO_2–TiO_2, and SiO_2–TiO_2–PbO gel-glasses,

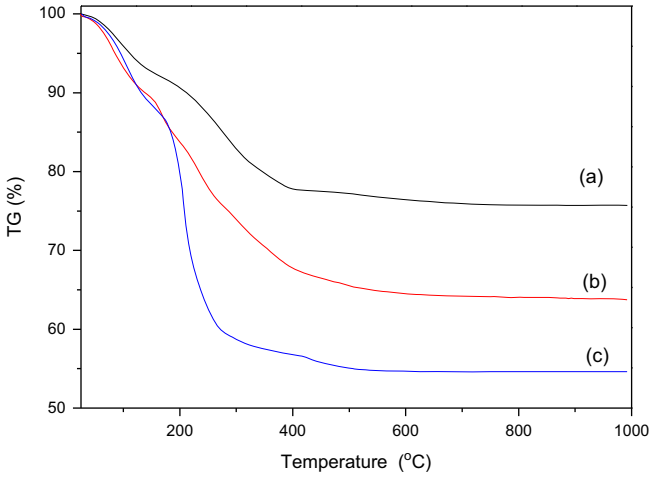

Fig. 4. TGA curves of the (a) SiO_2, (b) SiO_2–TiO_2, and (c) SiO_2–TiO_2–PbO gel-glasses.

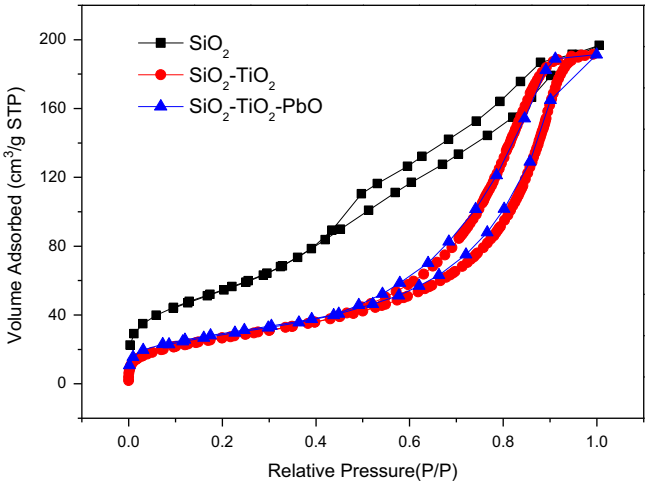

Fig. 5. N_2 adsorption–desorption isotherms of the (a) SiO_2, (b) SiO_2–TiO_2, and (c) SiO_2–TiO_2–PbO gel-glasses.

respectively, were observed, which can be attributed to the evaporation of the physically adsorbed water and ethanol. A subsequent sharp decrease in the weights of the SiO_2, SiO_2–TiO_2, and SiO_2–TiO_2–PbO gel-glasses to 15.14%, 23.58%, and 33.79%, respectively, occurred in the temperature range of 150 °C–400 °C. This decrease in weight ranges depends on the gel-glass composition. The weight loss in the second stage can be attributed to the thermal decomposition of particular organic solvents. During the synthesis procedure, wherein only DMF was included in the formation of SiO_2 gel-glass, additional acac was involved in the hydrolysis and condensation of SiO_2–TiO_2 gel-glass to restrain the rapid hydrolysis of TTIP. However, except for DMF and acac, 2-methoxyethanol anhydrous was used to dissolve $Pb(Ac)_2$ in the SiO_2–TiO_2–PbO gel-glass. Therefore, more weight was lost in the second stage when more organic solvents participated in the sol–gel process. In the third stage, which was conducted from 400 °C to 1000 °C, mass losses of approximately 2.43%, 3.52%, and 1.36% were observed in the SiO_2, SiO_2–TiO_2, and SiO_2–TiO_2–PbO gel-glasses, respectively. This mass loss can be attributed to the dehydration and evaporation of chemisorbed water.

3.3. Textural study

N_2 adsorption–desorption isotherms were used to provide details on the pore structures of the obtained gel-glasses, as shown in Fig. 5. All of the samples with different compositions exhibited a typical IV isotherm (definition by IUPAC), which is characteristic of mesoporous materials [15]. The appearance of H2 hysteresis loops at relative pressures indicates the presence of "ink-bottle"-type pores in these silica-based gel-glasses. Fig. 6 shows the pore distributions that were calculated using the Barrett–Joyner–Halenda (BJH) analysis of the desorption branch of type IV isotherms. A Brunauer–Emmett–Teller (BET) analysis of the type IV adsorption isotherms was conducted to estimate the specific surface area of the corresponding samples [15]. The cumulative pore volume in the mesopore range and

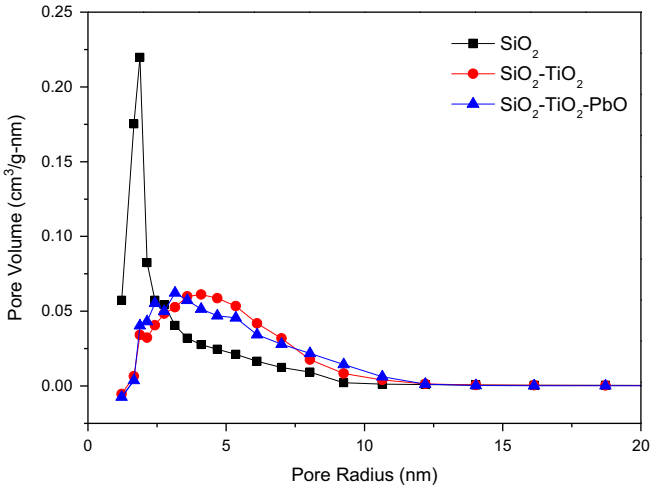

Fig. 6. Pore size distribution of the (a) SiO_2, (b) SiO_2–TiO_2, and (c) SiO_2–TiO_2–PbO gel-glasses.

the average mesopore diameter were calculated from the BJH analysis [15]. The results are summarized in Table 1.

In Fig. 6, the pore distributions of the three gel-glasses exhibited significant differences. The pore size distribution in the SiO_2 gel-glass was narrow and concentrated at approximately 1.8 nm. The pore size distribution in the SiO_2–TiO_2 gel-glass became broad and two grades of pore size were observed. The first grade was concentrated at 1.8 nm, and the other was concentrated at approximately 4.0 nm. In the SiO_2–TiO_2–PbO gel-glass, the dominant pore shifted slightly to dimensions smaller than of the SiO_2–TiO_2 gel-glass and contained a broad shoulder at 1.8 nm. The results in Table 1 show that the introduction of Ti^{4+} and Pb^{2+} decreased the specific surface area and pore volume but moderately increased the average pore size of the gel-glasses.

The changes discussed above suggest that the composition significantly influences the pore structure of silica-based gel-glasses. In our previous study, we proved that the pores in sol–gel-derived glasses correspond to the interspacing of gel

Table 1
BET specific surface values, pore volume, and average pore size of the SiO_2, SiO_2–TiO_2, and SiO_2–TiO_2–PbO gel-glasses.

Sample	BET surface area (m^2/g)	Pore volume (cm^3/g)	Average pore size (nm)
SiO_2	206.77	0.3030	1.88
SiO_2–TiO_2	100.58	0.2962	3.87
SiO_2–TiO_2–PbO	101.61	0.2958	3.23

granules formed by the hydrolysis and poly-condensation of metal alkoxides [16,17]. Therefore, the pores centered at 1.8 nm in the SiO_2 gel-glass can be attributed to the interspaces formed by SiO_2 granules during the hydrolysis and poly-condensation of TEOS, which are also present in the SiO_2–TiO_2 and SiO_2–TiO_2–PbO gel-glasses. Aside from the pores induced by the SiO_2 granules, a larger grade pore was found in the SiO_2–TiO_2 gel-glass, which confirms the formation of a bimodal distribution of pore shapes and dimensions. This larger grade pore can be attributed to the introduction of TiO_2 granules, in which the radius of Ti^{4+} is much larger than that of Si^{4+}, which results in larger interspaces in the TiO_2 granules. In addition, the presence of TTIP in the precursor, whose hydrolysis and poly-condensation rates are much faster than those of TEOS, would induce the silica granules to grow around the formed TiO_2 granules through inhomogeneous nucleation. In this condition, silica granules can grow further and form bigger granules. Thus, except for the pores at 1.8 nm, the TiO_2 and SiO_2 granules growing from the TiO_2 crystal nucleus, which are significantly bigger than the granules in the SiO_2 gel-glass (as confirmed by the SEM image in Fig. 1(b)), result in pores at 4.0 nm in the SiO_2–TiO_2 gel-glass, which consequently increase the average pore size and decrease the specific surface area. The slight decrease in pore volume can be attributed to the denser packing in the SiO_2–TiO_2 gel-glass. The SiO_2–TiO_2–PbO and SiO_2–TiO_2 gel-glasses had similar pore size distribution. A previous work has shown that lead oxide and silica can form glasses in any concentration in the binary system and that lead can function in glasses as its own network former or as modifier of the SiO_2 network. Experimental results have shown that the molar ratio of PbO to SiO_2 in the system was less than 0.3 and that PbO function as a network former and are included in the SiO_2 network. The molar ratio of PbO to SiO_2 was greater than 0.3 and they made their own chains [18]. In our present experimental conditions, a molar ratio of PbO to SiO_2 of 0.125 was calculated, which is less than 0.3, which indicates that PbO was involved in the formation of the silica network. Pb seemed to be partially clustered to form a PbO-like structure and was partially inserted into the SiO_2–TiO_2 matrix. The filled effect slightly decreased the pore volume and average pore size of SiO_2–TiO_2–PbO gel-glass, which is lower compared with those of the SiO_2–TiO_2 gel-glass.

3.4. Optical limiting study

The OL properties of the obtained gel-glasses were investigated via the open Z-scan method. Fig. 7 shows the 532 nm open aperture Z-scan results of the three gel-glass samples. The profile of the open Z-scan curve in SiO_2 gel-glass was a quasi-line parallel to the x-axis as expected, which implies that a single SiO_2 does not present an OL signature. However, for the SiO_2–TiO_2 and SiO_2–TiO_2–PbO gel-glasses, the normalized transmittance decreased from 100% to several tens percent when they moved toward the focal point. This characteristic is typical of OL materials. Thus, the appearance of the OL phenomenon is induced by TiO_2. Furthermore, no significant difference between the two valley-curves was observed. Both valley-curves exhibited a strong and symmetric loss of transmittance around $Z=0$, which could be a signature of either nonlinear absorption or nonlinear scattering. Comparing the curve profiles of the SiO_2–TiO_2 and SiO_2–TiO_2–PbO gel-glasses, the latter exhibited a deeper valley than the former, which indicates that the latter had stronger OL effect than the former. Therefore, aside from TiO_2, PbO is also the cause of nonlinear performance in the SiO_2–TiO_2–PbO gel-glass.

Several mechanisms, including nonlinear absorption (NLA) (e.g., excited-state, two-photon, multi-photon, and free-carrier absorption), nonlinear refraction (NLR), and nonlinear scattering (NLS), may contribute to OL [19]. Previous studies have proven that the nonlinear optical behaviors of TiO_2 that contain nanocomposites mainly originate from two-photon absorption (TPA) [20–22]. In the present study, the experimental data were fitted with a TPA process to verify the mechanisms. The normalized transmittance for the open-aperture Z-scan is given by [20]:

$$T(z) = \frac{C(1+z^2/z_0^2)}{\sqrt{\pi}\beta I_0 L_{eff}} \int_{-\infty}^{\infty} \ln(1+q_0 e^{-t^2}) dt, \quad (1)$$

where $z_0 = \omega_0^2/\lambda$ is the diffraction length of the Gaussian beam, ω_0 is the beam's waist radius, C is a normalization constant, $L_{eff} = [1-\exp(-\alpha_0 l)]/\alpha_0$ with α_0 is a linear absorption coefficient with l as the sample thickness, and L_{eff} is the effective thickness of the sample. I_0 is the intensity of the laser beam at the focus and $q_0 = \beta I_0 L_{eff}/(1+z^2/z_0^2)$. The total nonlinear absorption coefficient (β) can be determined by fitting Eq. (1) with the experimental data of the open aperture Z-scan. The β values of the SiO_2–TiO_2 and SiO_2–TiO_2–PbO gel-glasses of 0.17 and 0.26 cm/GW, respectively, were extracted from the best fit. The theory of TPA process fitted well with the experimental curves, which further confirms that TPA might be the key OL mechanism in the SiO_2–TiO_2 and SiO_2–TiO_2–PbO gel-glasses. However, the calculated β was significantly lower compared with those of TiO_2–PMMA nanohybrid and ZnO–TiO_2–SiO_2 nanocomposites [20,21]. Such a large difference was anticipated because of the

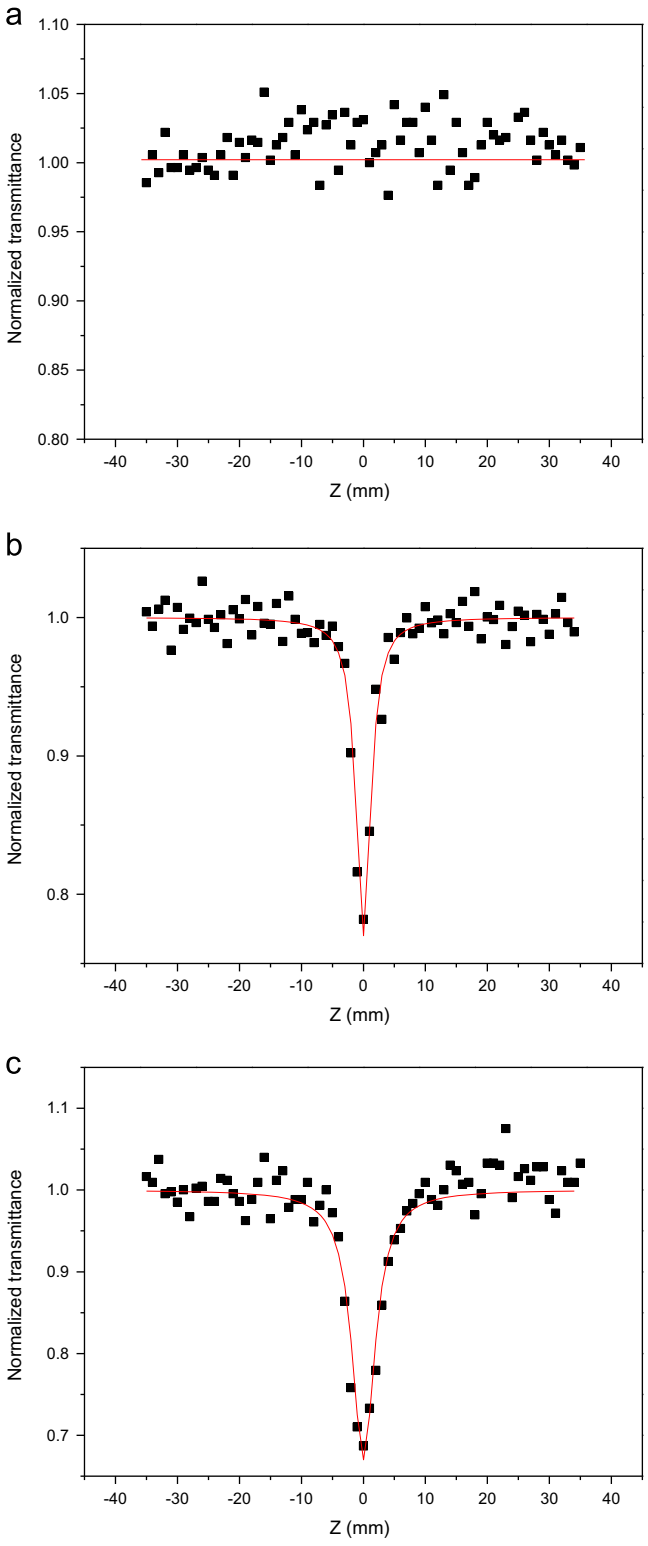

Fig. 7. Results of the open-aperture Z-scan for the (a) SiO_2, (b) SiO_2–TiO_2, and (c) SiO_2–TiO_2–PbO gel-glasses at 532 nm.

following two reasons: (1) the additive volumes of TTIP and $Pb(Ac)_2$ in the precursor were significantly lower than that of TEOS, which resulted in the low volume fraction of TiO_2 and PbO in the obtained gel-glasses; (2) the SiO_2–TiO_2 and SiO_2–TiO_2–PbO gel-glasses derived from the sol–gel technique

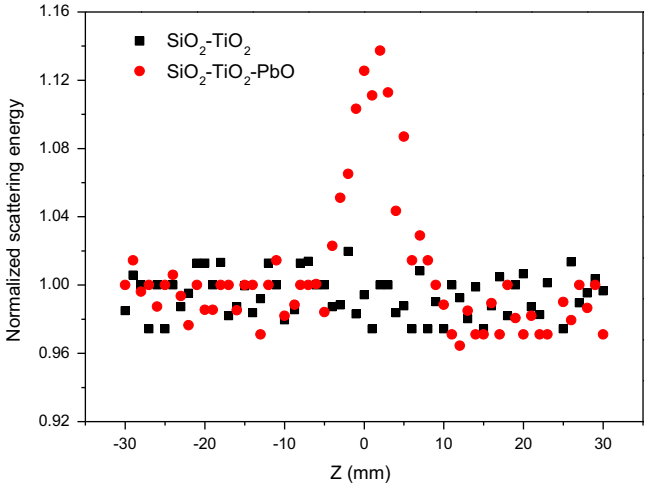

Fig. 8. Typical nonlinear scattering results of the SiO_2–TiO_2 and SiO_2–TiO_2–PbO gel-glasses at 532 nm. The energy detector was located at an angle of 45° from the axis.

without any annealing treatment were amorphous. Ji Wei et al. proved that crystallinity significantly influences the nonlinear optical properties of TiO_2. A high crystallinity would generally enhance the nonlinear absorption coefficient and nonlinear refractive index of the TiO_2–PMMA nanohybrid [20]. However, the nonlinear absorption coefficients in the SiO_2–TiO_2 and SiO_2–TiO_2–PbO gel-glasses were comparable with those of the Bi_2O_3–GeO_2–TiO_2 and Bi_2O_3–B_2O_3–TiO_2 ternary glasses, as reported by Chen Feifei's group [23,24]. In their work, the ternary glasses were synthesized at a temperature as high as 1200 °C via the melting method. Such glasses are often used for applications in the field of nonlinear optics and are not suitable matrices that can encapsulate other OL materials because most OL molecules would lose their activities at such temperature.

Given that the valleys in the open aperture Z-scan curves could be signatures of either nonlinear absorption or nonlinear scattering, an experiment involving NLS measurements was performed to determine if NLS contributes to the observed OL effects in SiO_2–TiO_2 and SiO_2–TiO_2–PbO gel-glasses. Fig. 8 shows the typical NLS results monitored at an angle of 45° from the laser axis. In the figure, the SiO_2–TiO_2–PbO gel-glass exhibited a significant scattering peak that was symmetric about the focus, which indicates the existence of NLS. However, no NLS peak was observed in the SiO_2–TiO_2 gel-glass, which implies that NLS did not have any contribution. In general, NLS in OL materials originates from microplasmas and solvent microbubbles in suspensions containing nano-size matter, such as carbon nanotubes, metal nanoparticles, and semiconductor nanoparticles, among others. Thus, investigating the NLS detected in the SiO_2–TiO_2–PbO gel-glass is of great interest because the rigid solid-state environment often precludes the formation of microbubbles. Consequently, the NLS behavior of the SiO_2–TiO_2–PbO gel-glass originates from PbO, which makes the SiO_2–TiO_2–PbO gel-glass have better OL performance than the SiO_2–TiO_2 gel-glass. Details of the scattering mechanisms merit further investigation, which is currently being conducted in our laboratory.

4. Conclusion

Two kinds of multicomponent inorganic gel-glasses, namely, SiO_2–TiO_2 binary and SiO_2–TiO_2–PbO ternary gel-glasses, were obtained via the hydrolysis and co-condensation of TEOS, TTIP, and $Pb(Ac)_2$. XRD, SEM, FT-IR spectroscopy, TGA, and pore structure measurements were performed to investigate the morphology, structure, and texture properties of the gel-glasses. The samples were mainly composed of amorphous phase without any detected phase separation. The intensity of the bands induced via Si–O–Si vibration in the SiO_2 gel-glass was lower compared with those of the SiO_2–TiO_2 and SiO_2–TiO_2–PbO gel-glasses, which indicates that the introduced Ti^{4+} and Pb^{2+} were partially involved in the hydrolysis and condensation processes. Furthermore, the composition significantly influenced the pore structure of silica-based gel-glasses, and the introduction of TiO_2 in the gel-glasses was responsible for the formation of bimodal-distributed pore shapes and dimensions in the multicomponent inorganic gel-glasses. The OL properties were measured at 532 nm via the open aperture Z-scan technique. The SiO_2–TiO_2 binary and SiO_2–TiO_2–PbO ternary gel-glasses exhibited greatly enhanced OL behaviors than the unitary SiO_2 gel-glass. The observed OL phenomenon in the SiO_2–TiO_2 binary gel-glass originated from two-photon absorption, whereas the TPA followed by nonlinear scattering contributed to the increased OL performance of the SiO_2–TiO_2–PbO ternary gel-glass. SiO_2–TiO_2 binary and SiO_2–TiO_2–PbO ternary gel-glasses are potential materials for practical applications in the fields of optics, all-optical switching, and related optical devices.

Acknowledgments

This work was supported by the National Natural Science Foundation of China (Grant no. 61108056) and Natural Science Foundation of Fujian Province (Grant no. 2012J01186).

References

[1] L. Tutt, A. Kost, Optical limitng performance of C_{60} and C_{70} solution, Nature 356 (1992) 255–256.
[2] M. Calvete, G.Y. Yang, Hanack, Porphyrins and phthalocyanines as materials for optical limiting, Synth. Met. 141 (2004) 231–243.
[3] J. Wang, Y. Chen, W.J. Blau, Carbon nanotubes and nanotube composites for nonlinear optical devices, J. Mater. Chem. 19 (2009) 7425–7443.
[4] S.S. Chu, S.F. Wang, Q.H. Gong, Ultrafast third-order nonlinear optical properties of graphene in aqueous solution and polyvinyl alcohol film, Chem. Phys. Lett. 523 (2012) 104–106.
[5] Y.H. Lee, Y.L. Yan, L. Polavarapu, Q.H. Xu, Nonlinear optical switching behavior of Au nanocubes and nano-octahedra investigated by femtosecond Z-scan measurements, Appl. Phys. Lett. 95 (2009) 023105.
[6] R.A. Ganeev, A.I. Ryasnyanskiy, T. Usmanov, Optical and nonlinear optical characteristics of the Ge and GaAs nanoparticle suspensions prepared by laser ablation, Opt. Commun. 272 (2007) 242–246.
[7] H.B. Zhan, W.Z. Chen, M.Q. Wang, C.L. Zou, C. Zheng, Optical limiting properties of peripherally modified palladium phthalocyanines doped silica gel glass, Chem. Phys. Lett. 389 (2004) 119–123.
[8] C. Zheng, M. Feng, Y.H. Du, H.B. Zhan, Synthesis and third-order nonlinear optical properties of a multiwalled carbon nanotube–organically modified silicate nanohybrid gel glass, Carbon 47 (2009) 889–2897.
[9] C. Zheng, Y.H. Du, M. Feng, H.B. Zhan, Shape dependence of nonlinear optical behavior of nanostructured silver and their silica gel glass composites, Appl. Phys. Lett. 93 (2008) 143108.
[10] M. Sheik-Bahae, A.A. Said, T.-H. Wei, D.J. Hagan, E.W.V. Stryland, Sensitive measurement of optical nonlinearities using single beam, IEEE J. Quantum Electron. 26 (1990) 760–769.
[11] A. Fidalgo, R. Ciriminna, L.M. Iharco, M. Pagliaro, Role of the alkyl − alkoxide precursor on the structure and catalytic properties of hybrid sol − gel catalysts, Chem. Mater. 17 (2005) 6686–6694.
[12] W. Que, Y. Zhou, Y.L. Lam, Y.C. Chan, S.D. Cheng, Z. Sun, C.H. Kam., Microstructural and spectroscopic studies of sol–gel derived silica-titania waveguides, J. Sol–Gel Sci. Technol. 18 (2000) 77–83.
[13] F. Farges, Coordination of Ti in crystalline and glassy fresnoites: a high-resolution XANES spectroscopy study at the Ti K-edge, J. Non-Cryst. Solids 204 (1996) 53–64.
[14] I. Ardelean, S. Lupsor, D. Rusu, Structural investigation of xMnO · $(100-x)[As_2O_3 \cdot PbO]$ glass system by FT-IR and Raman spectroscopies, Solid State Sci. 10 (2008) 1384–1386.
[15] S.J. Cregg, K.S.W. Sing, Adsorption, Surface Area and Porosity, second ed., Academic Press, London, 1982.
[16] M.D. Curran, A.E. Stiegman, Morphology and pore structure of silica xerogels made at low pH, J. Non-Cryst. Solids 249 (1999) 62–68.
[17] M.T. Colomer, M.A. Anderson, High porosity silica xerogels prepared by a particulate sol–gel route: pore structure and proton conductivity, J. Non-Cryst. Solids 290 (2001) 93–104.
[18] A.M. Zahra, C.Y. Zahra, B. Piriou., DSC and Raman studies of lead borate and lead silicate glasses, J. Non-Cryst. Solids 155 (1993) 45–55.
[19] L.W. Tutt, T.F. Boggess, A review of optical limiting mechanisms and devices using organics, fullerenes, semiconductors and other materials, Prog. Quantum Electron. 17 (1993) 299–338.
[20] A.H. Yuwono, J.M. Xue, J. Wang., Transparent TiO_2–PMMA nanohybrids of high nanocrystallinity and enhanced nonlinear optical properties, J. Nonlinear Opt. Phys. Mater. 14 (2005) 281–297.
[21] L. Irimpan, B. Kishnan, V.P.N. Nampoori, P. Radhakrishnan, Nonlinear optical characteristic of nanocomposites of ZnO–TiO_2–SiO_2, Opt. Mater. 31 (2008) 361–365.
[22] H.I. Elim, W. Ji, A.H. Yuwono, J.M. Xue, J. Wang, Ultrafast optical nonlinearity in poly (methylmethacrylate)–TiO_2 nanocomposites, Appl. Phys. Lett. 82 (2003) 2691–2693.
[23] F.F. Chen, B.A. Song, C.G. Lin, S.X. Dai, J.W. Cheng, J. Heo, Glass formation and third-order optical nonlinear characteristics of brismuthate glasses within Bi_2O_3–GeO_2–TiO_2 pseudo-ternary system, Mater. Chem. Phys. 135 (2012) 73–79.
[24] T.F. Xu, F.F. Chen, S.X. Dai, Q.H. Nie, X. Shen, X.S. Wang, Third-order optical nonlinear characterization of Bi_2O_3–B_2O_3–TiO_2 ternary glasses, Physica B 404 (2009) 2012–2015.